CHAPTER 3 EXPERIMENTAL APPARATUS

The experimental setup will be described in detail within this section. The entire system consisted several sub-systems that include the refrigerant flow loop, the ethylene–glycol/water flow loop, the test section, and the data acquisition, which are described further below.

3.1 Flow loop

As shown in Fig. 3.1, the experimental apparatus used in this study is comprised of a refrigerant (or test loop) and ethylene–glycol/water loop. The ethylene–glycol/water loop consists of a vapor-compression system, a centrifugal pump, a variable area flow meter and a tank containing a RTD, serpentine coil, and a cartridge heater, in order to control for the desired temperatures. This loop is responsible for condensing and subcooling the working fluid in the refrigerant loop using a plate-type heat exchanger.

For the refrigerant loop, the fluid in the receiver tank was circulated through the closed loop using a variable-speed magnetic gear pump. To keep the refrigerant free of contaminants, the fluid flowed through a filter/drier before entering the Cariolis-type mass flow meter and the pre-heater. Using a direct electrical heating method for the pre-heater, the refrigerant was evaporated to reach the desired quality before entering the heat sink.

At the upstream pre-heater, a sight glass was installed to observe the state of the refrigerant. In order to accurately estimate the liquid enthalpy at this point, the state of the refrigerant must be a single-phase liquid. A second sight glass was installed downstream of the pre-heater, with the same purpose of the previous one. These sight glasses were made of an electrically-resistant material, in order to isolate the electricity, which is directly supplied to the pre-heater.

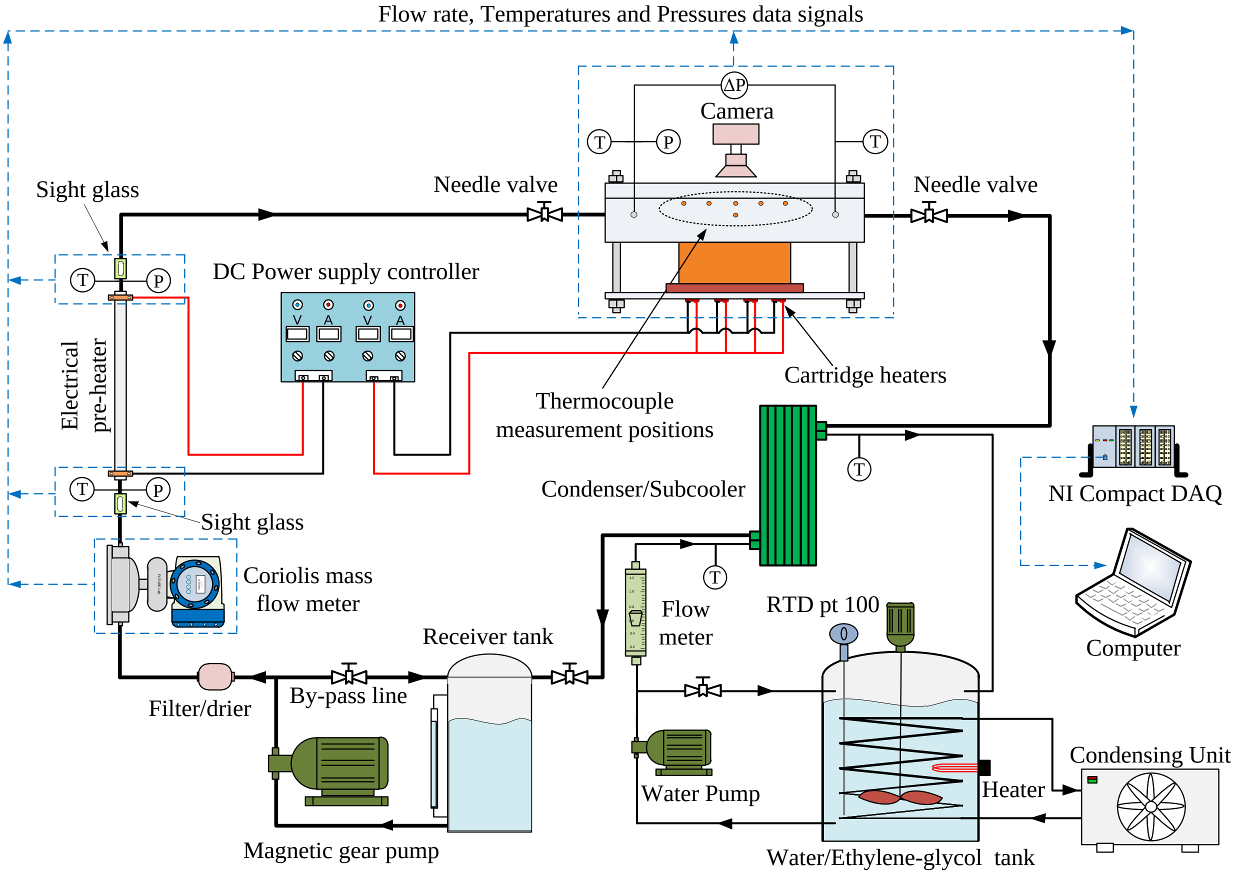

Figure 3.1 Schematic diagram of the flow boiling experimental apparatus

For the evaporation at the test section, a certain heat flux was conducted from a DC power supply controller. Finally, the refrigerant leaving the test section was condensed and subcooled inside the plate-type heat exchanger and returned to the receiving tank, thus closing the loop. Measuring instruments are installed at several locations, as shown in Fig. 3.1, to monitor the state of the refrigerant. All of the signals from the thermocouples, pressure transducer, and flow meter were recorded using Labview and the National Instruments DAQ system.

3.2 Test Section

Figure 3.2 shows an exploded view of the test section assembly. The primary components consist of top and bottom stainless support plates to provide the stress distribution act on the test section. A transparent polycarbonate plate was used to allow visualization of the flow. It was grooved to fit a rubber seal, in order to prevent leakage. A thin urethane sheet was placed on top of the microchannels of the heat sink, in order to preclude fluid cross-leakage between the channels. Epoxy resin (G-10) was selected for the housing, due to its good mechanical properties for this experiment. It has a low thermal conductivity (0.288 W/m K) and good resistance to R134a, and is fire-resistant and easy to machine.

The microchannel heat sink was fabricated from a copper block with 27 parallel rectangular channels, as shown in Fig. 3.3. Using a microscopic vision system, the channel depth, width, and fin thickness were measured at many locations along the channel, in order to determine the average dimensions of the channels. Each microchannel had a depth of 470 µm, a channel width of 382 µm, a wall thickness of 416 µm and a length of 40 mm. Corresponding to the parameters shown in Fig. 3.4, the important dimensional parameters that are useful for calculation are compiled in Table 3.1.

Twelve cartridge heaters were installed vertically in the bottom of the heat sink to heat the test section with a maximum power of 2.4 kW. The electrical power input to the cartridge heaters was controlled manually by a DC power supply controller unit. The quantity of electrical power was measured with a Clamp-On power meter (YOKOGAWA CW10 model), which has an uncertainty of ±2.2%. The 12 T-type thermocouples with diameters of 0.5 mm were inserted below the bottom of the channel wall to determine the temperature gradient and surface temperature at five locations along the length of the channel.

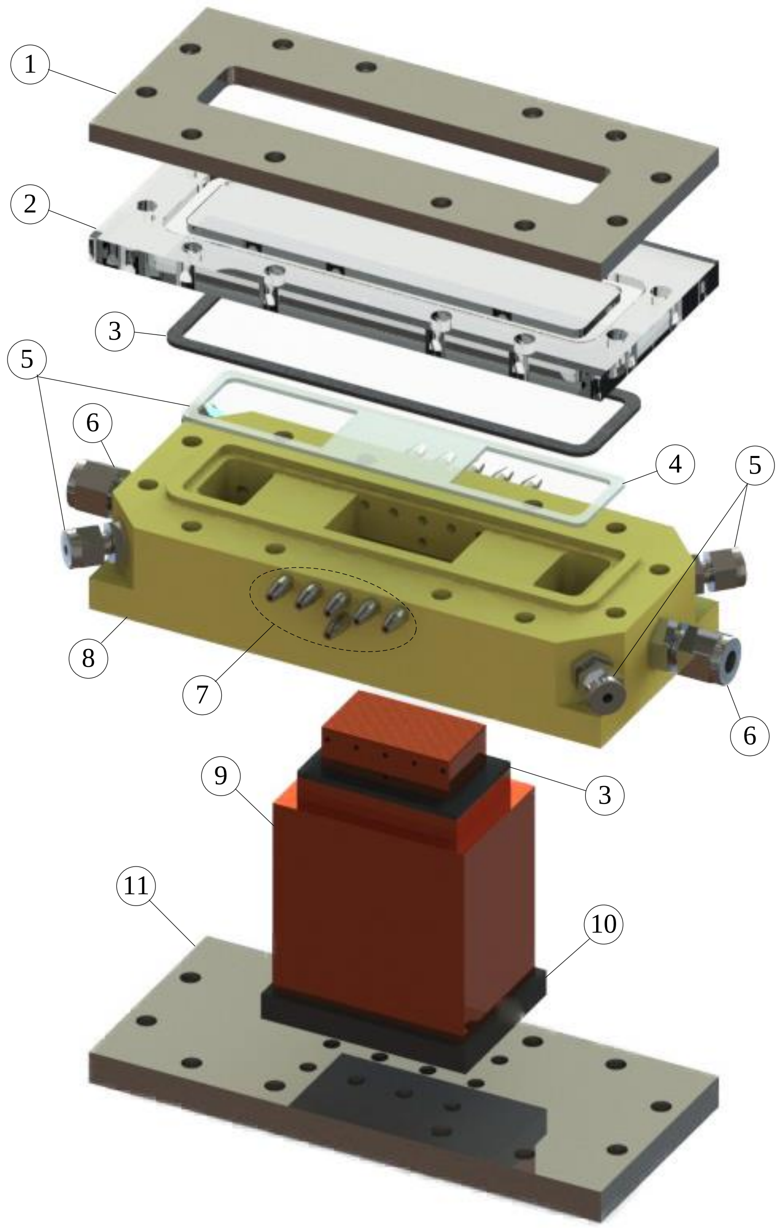

Figure 3.2 The exploded view of the test section consists of: (1) Stainless top plate, (2) Ttransparent polycarbonate plate, (3) Rubber seal, (4) Urethane thin sheet, (5) Thermocouple and pressure transducer connector ports, (6) Inlet and outlet connector ports, (7) Thermocouple connector ports, (8) G-10 housing, (9) Microchannels test piece, (10) Insulator plate and (11) Stainless bottom plate.

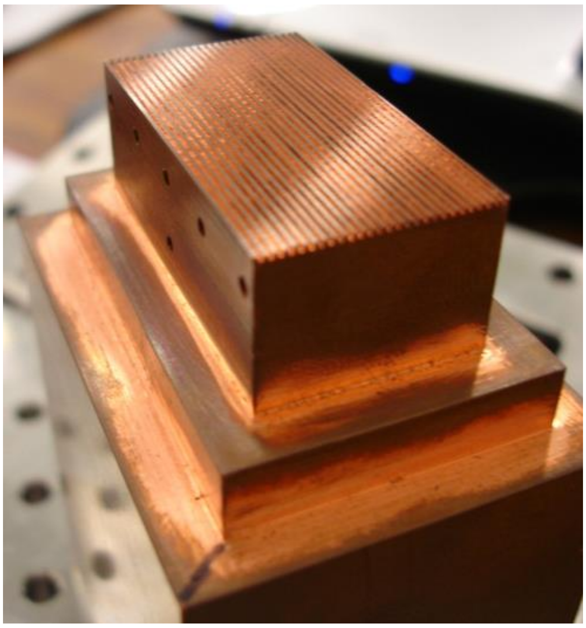

Figure 3.3 A photograph of the test piece

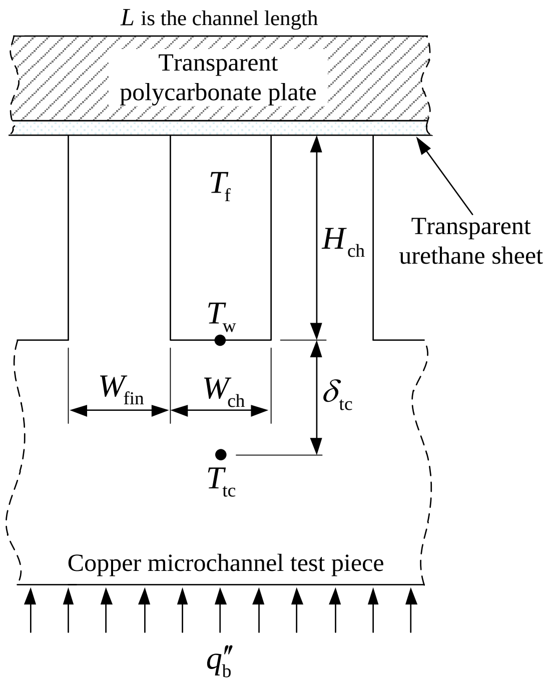

Figure 3.4 Schematic details of microchannel

Table 3.1 Dimensional details of the microchannels test piece

Dimensions	**Measurement**
Number of channels, N	27
Hydraulic diameter, D_h (μm)	421
Chanel width, W_{ch} (μm)	382
Chanel depth, H_{ch} (μm)	470
Fin thickness, W_{fin} (μm)	416
Aspect ratio $(\beta = H_{ch} / W_{ch})$	1.23
Chanel length, L (mm)	40
Distance from thermocouple to the channel base, δ_{tc} (mm)	3

The thermocouples' placement details are shown in Fig. 3.5. T-type thermocouples and pressure sensors were also located at the inlet and outlet of the microchannels to directly measure the local refrigerant temperature and pressure drop along the microchannels. In order to reduce heat loss to the surroundings, polyurethane (PU) foam was used as pre-insulation, due to its very high insulating properties, low thermal conductivity (approximate 0.022 W/m K), fire-resistance, light weight, and strength.

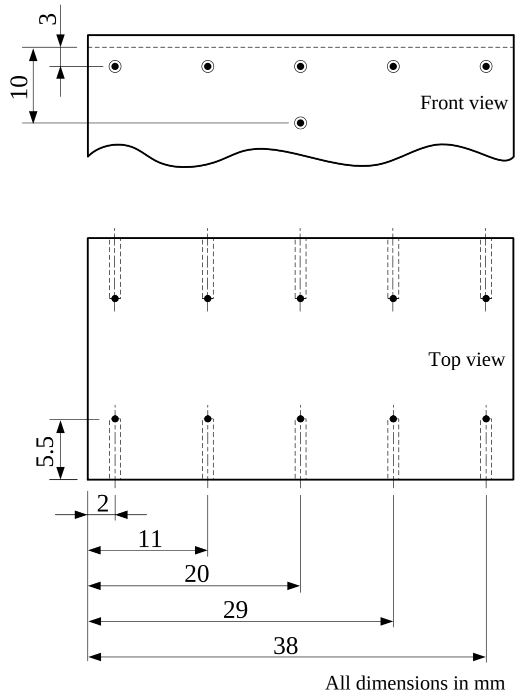

Figure 3.5 Thermocouple placement positions in the copper test piece

In this work, the experiments were conducted using varying heats to the test section in small increments, while the refrigerant flow rate, the saturation temperature, and the inlet vapor quality were kept constant at the desired values. The system is allowed to approach a steady state before the relevant data are recorded for several minutes. During the experiment, the temperatures are continuously recorded along the test section by the data logger. The profiles of the temperature help us to know the limit of useful data because a large increase in wall temperature and outlet saturation temperature is observed when dry-out occurs. The range of experimental conditions is listed in Table 3.2. And the uncertainties in the measured quantities and calculated parameters are presented in the Table 3.3.

Table 3.2 An experimental operating conditions

Experimental parameter	**Range**	**Unit**
Inlet quality, x_{in}	0.05-0.93	[-]
Saturation temperature, T_{sat}	13-23	^{o}C
Mass flux, G	400-1200	kg/m^2 s
Wall heat flux, q''_w	14.3 -168.4	kW/m^2

Table 3.3 Experimental uncertainties for measured parameters

Parameters	**Uncertainty**
Temperature	±0.1
Refrigerant mass flow rate	±0.035%
Wall heat flux	±2.20%
Inlet vapor quality	±6.87%
Average heat transfer coefficient	±4.36%
Frictional pressure gradient	±4.54%

3.3 Data Acquisition

A high speed data acquisition system (DAQ) was used to monitor and obtain data from the entire system. National Instruments brand DAQ is used. The Compact DAQ model high-speed signal conditioning products are used to acquire the high-speed data from the measurement. A LabVIEW was programmed to control the DAQ hardware. The LabVIEW Front Panel is included in Appendix B.